A&A 471, 151–158 (2007)
DOI: 10.1051/0004-6361:20077714

Astronomy & Astrophysics

The contribution of oxygen-neon white dwarfs to the MACHO content of the Galactic halo

J. Camacho[1], S. Torres[1,2], J. Isern[2,3], L. G. Althaus[4,5] and E. García-Berro[1,2]

[1] Departament de Física Aplicada, Escola Politécnica Superior de Castelldefels, Universitat Politècnica de Catalunya, Avda. del Canal Olímpic s/n, 08860 Castelldefels, Spain
e-mail: garcia@fa.upc.es
[2] Institute for Space Studies of Catalonia, c/Gran Capità 2–4, Edif. Nexus 104, 08034 Barcelona, Spain
[3] Institut de Ciències de l'Espai, CSIC, Campus UAB, Facultat de Ciències, Torre C-5, 08193 Bellaterra, Spain
[4] Facultad de Ciencias Astronómicas y Geofísicas, Universidad Nacional de La Plata, Paseo del Bosque s/n, 1900 La Plata, Argentina
[5] Instituto de Astrofísica La Plata, IALP, CONICET, Argentina

Received 25 April 2007 / Accepted 13 June 2007

ABSTRACT

Context. The interpretation of microlensing results towards the Large Magellanic Cloud (LMC) still remains controversial. White dwarfs have been proposed to explain these results and, hence, to contribute significantly to the mass budget of our Galaxy. However, several constraints on the role played by regular carbon-oxygen white dwarfs exist.
Aims. Massive white dwarfs are thought to be made of a mixture of oxygen and neon. Correspondingly, their cooling rate is larger than those of typical carbon-oxygen white dwarfs and they fade to invisibility in short timescales. Consequently, they constitute a good candidate for explaining the microlensing results.
Methods. Here, we examine in detail this hypothesis by using the most recent and up-to-date cooling tracks for massive white dwarfs and a Monte Carlo simulator which takes into account the most relevant Galactic inputs.
Results. We find that oxygen-neon white dwarfs cannot account for a substantial fraction of the microlensing depth towards the LMC, independently of the adopted initial mass function, although some microlensing events could be due to oxygen-neon white dwarfs.
Conclusions. The white dwarf population contributes at most a 5% to the mass of the Galactic halo.

Key words. stars: white dwarfs – stars: luminosity function, mass function – Galaxy: stellar content – Galaxy: structure – Galaxy: halo

1. Introduction

Several cosmological observations show compelling evidence that baryons represent only a small fraction of the total matter in our Universe and that non-baryonic dark matter dominates over baryons. To be specific, in the standard cosmological model $\Omega_\Lambda \simeq 0.72$ and $\Omega_M \simeq 0.27$, whereas $\Omega_B \simeq 0.044$. Moreover, most of the baryons are non–luminous, since $\Omega_\star \simeq 0.005$. For the case of our own Galaxy it has been found that the virial mass out to 100 kpc is $M \approx 10^{12}\,M_\odot$ while the baryonic mass in the form of stars is $M_\star \approx 7 \times 10^{10}\,M_\odot$, which means that for the Milky Way, the baryon fraction is at most 8% (Klypin et al. 2007). This problem is known as the missing bayon problem – see the excellent review of Silk (2007) for a complete, interesting and recent discussion of this issue – and it is critical in our understanding of how the Galaxy (an by extension other galaxies) were formed and will ultimately evolve. In order to solve this problem, three alternatives can be envisaged: either these baryons are in the outer regions of our Galaxy, or, perhaps, they never were present in the protogalaxy or, finally, they may have been ejected from the Milky Way. The most promising explanation and the currently favored one is the first of these options.

The most likely candidates for building up the baryonic dark matter density are massive baryonic halo objects, or MACHOs. It has been suggested that MACHOs could be planets ($M \sim 10^{-7}\,M_\odot$), brown dwarfs (with masses ranging from ~0.01 to ~0.1 $M_\odot$), primordial black holes ($M \gtrsim 10^{-16}\,M_\odot$), molecular clumps ($M \sim 1\,M_\odot$) and old white dwarfs ($M \sim 0.6\,M_\odot$). White dwarfs are specially interesting candidates not only because their intrinsic faintness, but also because in addition to the mass of the white dwarf itself their progenitors have to return to interstellar medium a sizeable fraction of their original mass (~2 $M_\odot$ on average) once the white dwarf is formed. Additionally, much expectation has been generated since the pioneering proposal of Paczyński (1986) that MACHOs could be found through gravitational microlensing. Since then, several groups such as the MACHO (Alcock et al. 1997, 2000), EROS (Lasserre et al. 2001; Goldman et al. 2002; Tisserand et al. 2006), OGLE (Udalski et al. 1994), MOA (Muraki et al. 1999) and SuperMACHO (Becker et al. 2005) teams have monitored millions of stars during several years in both the Large Magellanic Cloud (LMC) and the Small Magellanic Cloud (SMC) to search for microlensing events. Among these searches, it is worth mentioning that the MACHO collaboration has succeeded in revealing 13–17 microlensing events during their 5.7 yr analysis of 11.9 million stars in the LMC (Alcock et al. 2000). In their analysis they derived an optical depth towards the LMC of $\tau = 1.2^{+0.4}_{-0.3} \times 10^{-7}$ for events with durations in the range $2 < \hat{t} < 400$ days. This value is smaller than that expected for a full MACHO halo. In fact, it corresponds to a halo fraction $0.08 < f < 0.50$ at the 95% confidence level with a MACHO mass in the range $0.15\,M_\odot \leq M \leq 0.50\,M_\odot$, depending on the halo model. Despite the fact that only a fraction of the dark matter could be in the form of MACHOs, there is still a large controversy about the

nature of the reported microlensing events and to which extent they contribute to the mass budget of the dark halo of the Galaxy. In fact, a large variety of possible explanations have been proposed to explain these microlensing events. For instance, white dwarfs, brown dwarfs and black holes appear as natural candidates, whereas self–lensing by stars of the LMC (Sahu 1994; Gyuk et al. 2000) has been proposed as well. Also, other explanations – like tidal debris or a dwarf galaxy toward the LMC (Zhao 1998), a galactic extended shroud population of white dwarfs (Gates & Gyuk 2001), blending effects (Belokurov et al. 2003; 2004), non-conventional initial mass functions (Adams & Laughlin 1996; Chabrier et al. 1996), spatially varying mass functions (Kerins & Evans 1998; Rahvar 2005), and other explanations (Holopainen et al. 2006) – have been also thoroughly discussed during the last years. However, all of these proposals have been received with some criticism because none of them fully explains the observed microlensing results.

There are as well other observations that are important pieces of evidence in this puzzle, such as the results of the EROS collaboration or the search for very faint objects in the Hubble Deep Field. We briefly summarize them. The EROS team has recently presented an analysis of a subsample of bright stars from the LMC, minimizing the source confusion and blending effects (Tisserand et al. 2006). Their results imply that the optical depth towards the LMC is $\tau < 0.36 \times 10^{-7}$ at the 95% confidence level, corresponding to a fraction of halo mass of less than 7%. This result is 4 times smaller than that obtained by the MACHO team and, consequently, sets a strong upper bound to the contribution of MACHOs to the mass budget of the Galactic dark matter halo. Nevertheless, the nature of the observed microlensing events still remains to be clarified. Also, the Hubble Deep Field-South has provided another opportunity to test the contribution of white dwarfs to the Galactic dark matter. In particular, Kilic et al. (2005) have recently found three white dwarf candidates among several faint blue objects which exhibit significant proper motion and, thus, are assumed to belong to the thick-disk or the halo populations. If in the end these white dwarfs are spectroscopically confirmed it would imply that white dwarfs can account for about $\lesssim$10% of the Galactic dark matter, which would be consistent with the results of the EROS team, and with previous estimates (Chabrier 2004).

In a previous paper (García-Berro et al. 2004) we extensively analyzed the role played by the carbon-oxygen (CO) white dwarf population in several different observational results, namely, the reported microlensing events towards the Large Magellanic Cloud (Alcock et al. 2000), the results of the Hubble Deep Field (Ibata et al. 1999) and the results of the EROS experiment (Goldman et al. 2002). We performed a thorough study for a wide range of Galactic inputs, including different initial mass functions and halo ages, and several density profiles corresponding to different halo models. Our main result was that a sizeable fraction of the halo dark matter cannot be locked in the form of old hydrogen–rich white dwarfs with CO cores. Specifically, we found that this fraction should be of the order of 4%, in agreement with the standard models of the Galactic halo. However in our analysis we disregarded the contribution of massive white dwarfs, that is, stars more massive than $\sim$1.1 $M_{\odot}$. The core of these white dwarfs consists of a mixture of oxygen and neon. Since oxygen-neon (ONe) white dwarfs cool considerably faster than the bulk of CO white dwarfs (Althaus et al. 2007) it is reasonable to expect that perhaps some of the microlensing events could be due to these elusive massive white dwarfs. It is also worth mentioning at this point that the MACHO collaboration in their first season reported a microlensing event with a duration of 110 days towards the galactic bulge (Alcock et al. 1995). For this particular event a parallax could be obtained from the shape of the light curve, from which a mass of $1.3^{+1.3}_{-0.6}\,M_{\odot}$ was derived, indicating that the gravitational lens could possibly be a massive ONe white dwarf or a neutron star. Moreover, studies about the distribution of masses of the white dwarf population (Finley et al. 1997; Liebert et al. 2005) show the existence of a narrow sharp peak near 0.6 $M_{\odot}$, with a tail extending towards larger masses, with several white dwarfs with spectroscopically determined masses within the interval comprised between 1.0 and 1.2 $M_{\odot}$.

In this paper we analyze if ONe white dwarfs could be responsible for a sizeable fraction of the reported microlensing events towards the LMC. The paper is organized as follows. In Sect. 2 we briefly describe the main ingredients of our Monte Carlo code and other basic assumptions and procedures necessary to evaluate the microlensing optical depth towards the LMC. Section 3 is devoted to describe our main results, including the contribution of ONe white dwarfs to the halo white dwarf luminosity function and to the microlensing optical depth towards the LMC, and we compare our results to those of the MACHO and EROS teams. In this section we also check if ONe white dwarfs could be detected in the Hubble Deep Field South and we discuss the contribution of ONe white dwarfs to the baryonic content of the Galaxy. Finally, in Sect. 4 our major findings are summarized and we draw our conclusions.

2. The model

2.1. The Monte Carlo simulation

An extensive description of our Monte Carlo simulator has been already presented in García-Berro et al. (2004). Consequently, here we will only briefly summarize the main ingredients of our model. We have used a random number generator algorithm (James 1990) which provides a uniform probability density within the interval $(0, 1)$ and ensures a repetition period of $\gtrsim 10^{18}$, which is enough for our purposes. Each one of the Monte Carlo simulations discussed in Sect. 3 below consists of an ensemble of 40 independent realizations of the synthetic white dwarf population, for which the average of any observational quantity along with its corresponding standard deviation were computed. Here the standard deviation means the ensemble mean of the sample dispersions for a typical sample.

We have considered an otherwise typical spherically symmetric halo. The density profile of this model is the isothermal sphere of radius 5 kpc, also called the "S-model", which has been extensively used by the MACHO collaboration (Alcock et al. 2000; Griest 1991). Despite the existence of other density profiles, such as the exponential power-law model, the Navarro et al. (1997) density profile and others, in our previous study (García-Berro et al. 2004) we showed that the differences between them are not significant for the case under study and, consequently, we adopt the most simple description. The position of each synthetic star is randomly chosen according to this density profile.

We have considered two different initial mass functions, the rather standard initial mass function of Scalo (1998) and the biased log-normal initial mass function proposed by Adams & Laughlin (1996), which is very similar to the non-conventional initial mass function of Chabrier et al. (1996). This biased initial mass function has been included just for the sake of completeness, since it does not seem to be compatible with the observed properties of the halo white dwarf population (Isern et al. 1998;

García-Berro et al. 2004), with the contribution of thermonuclear supernovae to the metallicity of the Galactic halo (Canal et al. 1997), and with the observations of galactic halos in deep galaxy surveys (Charlot & Silk 1995). The main sequence mass is obtained by drawing a pseudo-random number according to the adopted IMF. Once the mass of the progenitor of the white dwarf is known we randomly choose the time at which each star was born. We assume that the halo was formed 14 Gyr ago in an intense burst of star formation of duration ~1 Gyr. Given the age of the halo, the time at which each main-sequence progenitor was born and the main sequence lifetime as a function of the mass in the main sequence (Iben & Laughlin 1989) we know which stars have had time enough to enter in the white dwarf cooling track, and given a set of theoretical cooling sequences and the initial to final mass relationship (Iben & Laughlin 1989), we know their luminosities, effective temperatures and colors. The cooling sequences adopted here depend on the mass of the white dwarf. White dwarfs with masses smaller than $M_{\rm WD} = 1.1\,M_{\odot}$ are expected to have a CO core and, consequently, for them we adopt the cooling tracks of Salaris et al. (2000). White dwarfs with masses larger than $M_{\rm WD} = 1.1\,M_{\odot}$ most probably have ONe cores and for these white dwarfs we adopt the most recent cooling sequences of Althaus et al. (2007). Both sets of cooling sequences incorporate the most accurate physical inputs for the stellar interior (including neutrinos, crystallization, phase separation and Debye cooling) and reproduce the blue turn at low luminosities (Hansen 1998). Also, the ensemble of cooling sequences used here encompass the full range of interest of white dwarf masses, so a complete coverage of the effects of the mass spectrum of the white dwarf population was taken into account.

The kinematical properties of the halo white dwarf population have been modeled according to a Gaussian law (Binney & Tremaine 1987):

$$f(v_r, v_t) = \frac{1}{(2\pi)^{3/2}} \frac{1}{\sigma_r \sigma_t^2} \exp\left[-\frac{1}{2}\left(\frac{v_r^2}{\sigma_t^2} + \frac{v_t^2}{\sigma_t^2}\right)\right] \tag{1}$$

where σ_r and σ_t – the radial and the tangential velocity dispersion, respectively – are related by the following expression:

$$\sigma_t^2 = \frac{V_{\rm c}^2}{2} + \left[1 - \frac{r^2}{a^2 + r^2}\right]\sigma_r^2 + \frac{r}{2}\frac{{\rm d}(\sigma_r^2)}{{\rm d}r} \tag{2}$$

which reproduces the flat rotation curve of our Galaxy at large distances. We have adopted a circular velocity $V_{\rm c} = 220\ {\rm km\,s^{-1}}$. Finally, and in order to obtain the heliocentric velocities we have taken into account the peculiar velocity of the Sun $(U_{\odot}, V_{\odot}, W_{\odot}) = (10.0, 15.0, 8.0)\ {\rm km\,s^{-1}}$ (Dehnen & Binney 1998). Since white dwarfs usually do not have determinations of the radial component of the velocity, the radial velocity is eliminated when a comparison with the observational data is needed. Moreover, we only consider stars with velocities larger than $250\ {\rm km\,s^{-1}}$ because white dwarfs with velocities smaller than this would not be considered as halo members. Additionally, we also discard stars with velocities larger than $750\ {\rm km\,s^{-1}}$, because they would have velocities exceeding 1.5 times the escape velocity.

2.2. Modeling the microlensing events towards the LMC

In order to ascertain the contribution of halo white dwarfs to the microlensing events towards the LMC we have proceeded in three steps. First of all we have built a model of the LMC following closely the procedures detailed in Gyuk et al. (2000) and Kallivayalil et al. (2006). This model takes into account, among other parameters, the scale length and scale height of the LMC, its inclination and its kinematical properties. This model provides us with a synthetic population of stars representative of the monitored point sources. In a second step we search for those halo white dwarfs that could be responsible of a microlensing event. This implies that the white dwarf should be fainter than a magnitude limit, otherwise it would not be considered as a genuine microlensing event. Typically we have taken $m_{\rm V}^{\rm cut} = 17.5^{\rm mag}$, which is the value adopted by Alcock et al. (2000). This value has been confirmed to be a reasonable estimate by the detailed theoretical simulations of García-Berro et al. (2004). Finally, we check if the angular distance between the white dwarf and the monitored star is smaller than the Einstein radius $\theta_{\rm E} = R_{\rm E}/D_{\rm OL}$, where $D_{\rm OL}$ is the distance between the observer and the lens and $R_{\rm E}$ is the Einstein radius which is given by the expression

$$R_{\rm E} = 2\sqrt{\frac{GMD_{\rm OS}}{c^2}x(1-x)} \tag{3}$$

where $D_{\rm OS}$ is the observer-source distance and $x \equiv D_{\rm OL}/D_{\rm OS}$. If this is the case then we have a microlensing event and we compute the corresponding probability. This probability is integrated over the total monitoring period of observation and filtered by the detection efficiency function, which allows us ot obtain the optical depth (Alcock et al. 2000):

$$\tau = \frac{1}{E}\frac{\pi}{4}\sum_i \frac{\hat{t}_i}{\varepsilon(\hat{t}_i)} \tag{4}$$

where E is the total exposure (in star-years), $\hat{t}_i$ is the Einstein ring diameter crossing time, and $\varepsilon(\hat{t}_i)$ is the detection efficiency. The detection efficiency and E depend on the particular characteristics of the experiment and, hence, we consider different detection efficiencies and different total exposures for the MACHO and EROS experiments. Specifically, for the case in which we analyze the results of the MACHO collaboration we have taken 1.1×10^7 stars during 5.7 yr and over 13.4 deg^2, whereas the detection efficiency has been modeled as:

$$\varepsilon(\hat{t}) = \begin{cases} 0.43\,{\rm e}^{-(\ln(\hat{t}/T_{\rm m}))^{3.58}/0.87}, & \hat{t} > T_{\rm m} \\ 0.43\,{\rm e}^{-|\ln(\hat{t}/T_{\rm m})|^{2.34}/11.16}, & \hat{t} < T_{\rm m} \end{cases} \tag{5}$$

where $T_{\rm m} = 250$ days. This expression provides a good fit to the results of Alcock et al. (2000). For the EROS experiment we have used 0.7×10^7 stars over a wider field of 84 deg^2 and over a period of 6.7 yr. Regarding the detection efficiency we have adopted a numerical fit to the results presented in Tisserand et al. (2006).

3. Results

3.1. The halo white dwarf luminosity function

Despite the increasing number of surveys searching for white dwarfs – like the Sloan Digital Sky Survey (Eisenstein et al. 2006), the 2 Micron All Sky Survey (Cutri et al. 2003), the SuperCosmos Sky Survey (Hambly et al 2001), the 2dF QSO Redshift Survey (Vennes et al. 2002), and others – their success in finding halo white dwarfs has been limited. Thus, the observational determination of the halo white dwarf luminosity is still today rather uncertain. In fact, the two attempts to build such a luminosity function (Liebert et al. 1989; Torres et al. 1998) have provided us only with the bright branch of the halo white dwarf luminosity function. Nevertheless, this is enough

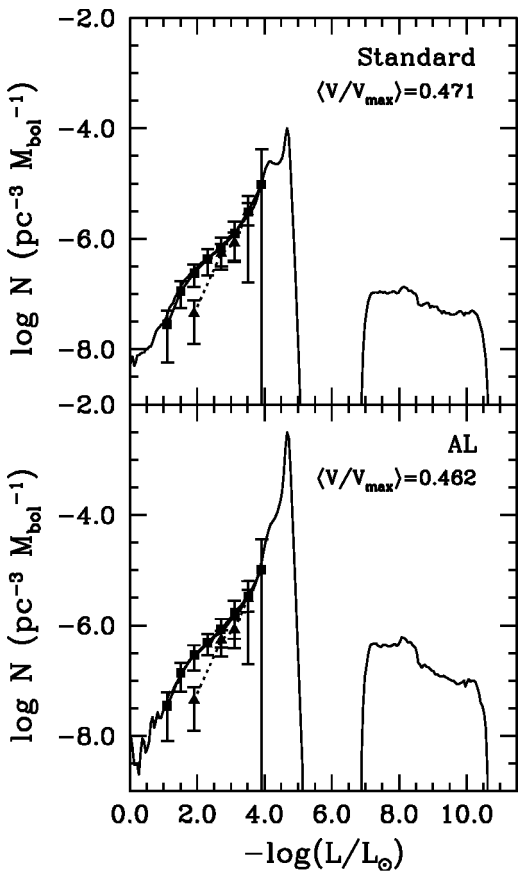

Fig. 1. Luminosity function of halo white dwarfs for a standard initial mass function (*top panel*) and a biased initial mass function (*bottom panel*). The observational luminosity function of halo white dwarfs is represented using a dotted line (Torres et al. 1998) and solid triangles, while the theoretical luminosity function is shown using a solid line and squares. See text for details.

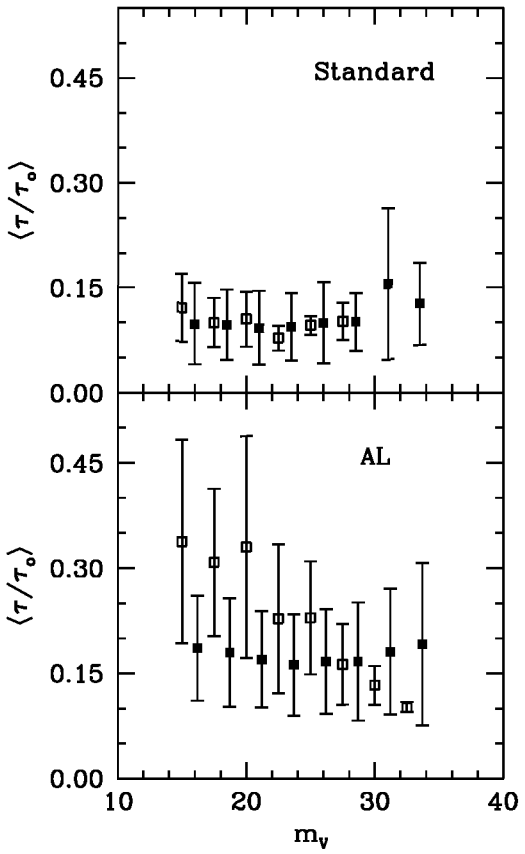

Fig. 2. Microlensing optical depth towards the LMC as a function of the limiting magnitude. Open and solid simbols represent the population of white dwarfs without and with the contribution of the ONe white dwarfs, respectively. The solid symbols have been shifted for the sake of clarity.

for our purposes, since we only need a normalization criterion and, hence, only an upper limit to the local density of moderately bright dwarfs is needed. Consequently, we have used the luminosity function of Torres et al. (1998) and we have normalized the local density of white dwarfs obtained from our Monte Carlo simulations to its observed value, $n \sim 9.0 \times 10^{-6}$ pc^{-3} for $\log(L/L_{\odot}) \gtrsim -3.5$ (Torres et al. 1998).

From the distribution of white dwarfs obtained using our Monte Carlo simulations we compute the white dwarf luminosity function using the $1/V_{\rm max}$ method (Schmidt 1968). It is important to mention that when deriving a luminosity function using the $1/V_{\rm max}$ method a proper motion cut and a limiting magnitude are required. The set of selection criteria adopted here for computing the halo white dwarf luminosity function is the same as used in García-Berro et al. (2004). Namely, we have chosen a limiting magnitude $m_{\rm V}^{\rm lim} = 17.5^{\rm mag}$ and a proper motion cut $\mu \geq 0.16''$ yr^{-1}. With all these inputs the luminosity functions in Fig. 1 are obtained. The top panel shows the halo white dwarf luminosity function obtained using a standard initial mass function, whereas the bottom panel shows the luminosity function when the biased initial mass function of Adams & Laughlin (1996) is adopted. The simulated luminosity functions are represented as squares connected with solid lines, whereas the observational luminosity function is represented as triangles connected with dashed lines. We also recall that, by construction, our samples are complete, although we only select about 10 white dwarfs using the selection criteria discussed before. However, our simulations do provide the whole population of white dwarfs, which is much larger. Hence, we can obtain the *real* luminosity function by simply counting white dwarfs in the computational volume. This is done for all realizations and then we obtain the average. The result is depicted as a solid line in Fig. 1. The true luminosity function steadily increases for luminosities larger than $\log(L/L_{\odot}) \simeq -5.0$ and then sharply drops. This drop-off is given by the paucity of CO white dwarfs with appropriate ages (14 Gyr). Note however that the bulk of the population of ONe white dwarfs is located at much smaller luminosities, a consequence of the much shorter cooling timescales of these white dwarfs. In fact, for a typical halo age of 14 Gyr, the bulk of the ONe white dwarf population has already entered the fast Debye cooling phase and, consequently, would not be detectable with the current observational facilities. In the next sections we explore if this elusive white dwarfs contribute significantly to the microlensing optical depth. It is also important to note that with the adopted limiting magnitude and proper motion cut we obtain simulated white dwarf luminosity functions which are totally compatible with the observational one. Hence, the inclusion of massive ONe white dwarfs does not appreciably change the resulting white dwarf luminosity function, which is very similar to that obtained in García-Berro et al. (2004).

3.2. Microlensing towards the LMC

Firt of all, we analyze the result obtained by the MACHO collaboration. In Fig. 2 we show the contribution to the optical depth towards the LMC due to the white dwarf population as

Table 1. Summary of the results obtained for the simulation of microlenses towards the LMC for the MACHO model for an age of the halo of 14 Gyr, different model IMFs, and several magnitude cuts.

	Standard				AL			
Magnitude	17.5	22.5	27.5	32.5	17.5	22.5	27.5	32.5
$\langle N_{\rm WD}\rangle$	0 ± 1	0 ± 1	0 ± 1	0 ± 1	3 ± 3	2 ± 2	1 ± 1	0 ± 2
$\langle m\rangle$ $(M/M_\odot)$	0.593	0.599	0.619	0.888	0.636	0.638	0.651	0.684
$\langle \mu\rangle$ ($''$ yr^{-1})	0.018	0.015	0.009	0.004	0.038	0.025	0.010	0.003
$\langle d\rangle$ (kpc)	2.85	3.52	6.27	14.65	1.31	2.22	5.45	18.73
$\langle V_{\rm tan}\rangle$ (km s^{-1})	238	243	262	268	240	260	257	279
$\langle \hat{t}_{\rm E}\rangle$ (d)	56.6	59.8	82.4	121.2	34.9	48.0	76.6	129.7
$\langle \tau/\tau_0\rangle$	0.139	0.134	0.187	0.131	0.180	0.162	0.167	0.192

a function of the adopted limiting magnitude. The results have been normalized to the value derived by Alcock et al. (2000), $\tau_0 = 1.2 \times 10^{-7}$. The open symbols represent the contribution if only CO white dwarfs are taken into account, while the solid symbols show the contribution to the microlensing optical depth when both CO and ONe white dwarfs are correctly included in the model white dwarf population. As can be seen, for none of the adopted initial mass functions the inclusion of the ONe white dwarf population significantly increases the contribution of white dwarfs to the microlensing optical depth towards the LMC, despite the fact that ONe white dwarfs are much fainter than regular CO white dwarfs (see also Fig. 1). Specifically, the contribution of the white dwarf population is, respectively, of the order of 10% for the case of the standard initial mass function and somewhat larger (~15%) for the log-normal initial mass function of Adams & Laughlin (1996). These figures are comparable to those already found in García-Berro et al. (2004). The only differences are that in the case of the standard mass function the contribution of ONe white dwarfs to the microlensing optical depth is clearly dominant only when the adopted limiting magnitude is of the order of 30, which is a totally unrealistic value. For the case of the log-normal initial mass function the results presented here show that the contribution is nearly constant, independently of the adopted limiting magnitude, whereas when only the contribution of CO white dwarfs was considered the contribution to the optical depth of the halo white dwarf population was clearly decreasing for increasing magnitude cuts.

A summary of the results obtained with our Monte Carlo simulator can be found in Table 1, where we show for four selected magnitude cuts the number of microlensing events, the average mass of the microlenses, their average proper motion, distance and tangential velocity, the corresponding Einstein crossing times and, finally, the contribution to the microlensing optical depth. It is important to discuss some of the numerical values in Table 1. For instance, it is clear that the larger the magnitude cut, the more massive the average mass of the lenses, as it should be expected from Fig. 1. In particular, for the case in which a standard initial mass function is used we obtain that for the largest limiting magnitude the average mass is ~0.9 $M_\odot$, indicating that in a sizeable fraction of the Monte Carlo realizations the lens is an ONe white dwarf. Also, the log-normal initial mass function produces more microlensing events, as one should expect, given that this biased initial mass funtion was tailored to produce more microlensing events. In fact for this initial mass function a maximum number of 6 microlensing events should be expected, while for the standard initial mass function we should expect 1 microlensing event, at most. However, the contribution to the microlensing optical depth is only slightly larger for the Adams & Laughlin (1996) initial mass function. The reason for this is that the microlensing events for this distribution have shorter Eintein crossing times, as seen in Table 1.

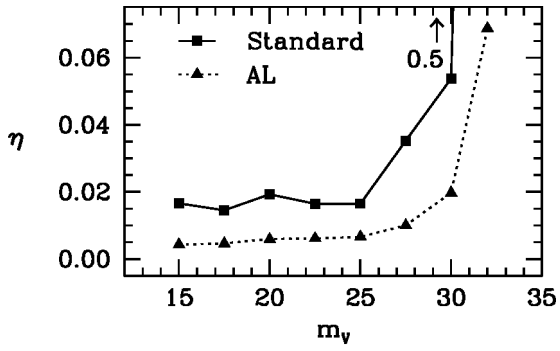

Fig. 3. Fraction of microlenses due to ONe white dwarfs with respect to the whole population of white dwarfs for the standard initial mass function – squares – and for the log-normal initial mass function of Adams & Laughlin (1996) – triangles.

The results obtained so far are not evident at first glance, since one may expect that ONe white dwarfs should be good microlensing candidates. As previously mentioned, ONe white dwarfs have a faster cooling rate than that of CO white dwarfs and, consequently, they reach much fainter magnitudes for the same cooling age. Hence, for reasonable halo ages one should naively expect that the probability that a ONe white dwarf could produce a microlensing event would be somewhat larger than that of a CO white dwarf, given that for reasonable halo ages practically all ONe white dwarfs have magnitudes larger than the magnitude cuts adopted here. However, even if this is indeed the case, we have shown that the total contribution of ONe white dwarfs is almost negligible. To clarify this result we have analyzed the fraction of microlenses due to ONe white dwarfs with respect to that of the total population. In Fig. 3 we show this fraction as a function of the limiting magnitude for the two initial mass functions under study. As can be seen, the contribution of ONe white dwarfs is small for limiting magnitudes below $25^{\rm mag}$. Specifically, for the case of the standard initial mass function they only contribute a modest 2%, whereas for the log-normal initial mass function the contribution is halved. This situation only reverses when magnitude cuts larger than $\sim 27^{\rm mag}$ are adopted. This result by itself is not explanatory of why the contribution of ONe white dwarfs is not significant. We recall here that the contribution of an object to the total optical depth is given by Eq. (4), which depends on the Einstein crossing time which, in turn, depends on the Einstein radius and on the transverse velocity of the lens, $t_{\rm E} = r_{\rm E}/v_{\rm tan}$. The Einstein radius scales as the root of the mass of the object and it also depends on the lens-object distance – see Eq. (3). We note that the average mass of an ONe white dwarf is larger than that of a CO white dwarf. Also, given the intrinsic faintness of ONe white dwarfs, their spatial distribution in the computational volume is different because we are selecting microlensing candidates with magnitudes

Table 2. Average values for the ONe white dwarf population.

	Standard				AL			
Magnitude	17.5	22.5	27.5	32.5	17.5	22.5	27.5	32.5
$\langle m \rangle$ $(M/M_\odot)$	1.118	1.106	1.244	1.130	1.092	1.082	1.083	1.101
$\langle d \rangle$ (kpc)	4.95	3.98	2.83	3.80	2.31	2.02	2.84	5.75
$\langle V_{\rm tan} \rangle$ (km s^{-1})	253	257	250	250	266	255	250	269
$\langle \hat{t}_{\rm E} \rangle$ (d)	107.9	91.6	77.7	104.1	56.8	61.6	75.0	99.0

fainter than a given limiting magnitude. Thus, it can be expected that the contribution to the optical depth of an representative object of the these two populations should be different as well.

In Table 2 we show the average parameters of the ONe white dwarf population susceptible to produce a microlensing event. The average mass of an ONe white dwarf is $\simeq 1.1\ M_\odot$, while for a CO white dwarf it is $\simeq 0.6\ M_\odot$. On the other hand, the average distance of ONe white dwarfs is in the range between about 2 and 4 kpc, independently of the limiting magnitude, while for the CO white dwarf population the average distance increases for increasing magnitude cuts. Finally, the average tangential velocities are very similar for all the magnitude cuts, given that the selection criteria are independent of the kinematical properties of the sample. With these data and using Eqs. (3) and (4) the ratio of the contribution to the optical depth of a typical ONe white dwarf with respect to the contribution of a typical CO white dwarf is

$$\frac{\tau_{\rm ONe}}{\tau_{\rm CO}} = \frac{\hat{t}_{\rm ONe}}{\hat{t}_{\rm CO}} \frac{\varepsilon(\hat{t}_{\rm CO})}{\varepsilon(\hat{t}_{\rm ONe})} \approx \sqrt{\frac{M_{\rm ONe} D_{\rm OL}^{\rm ONe}}{M_{\rm CO} D_{\rm OL}^{\rm CO}}} \frac{\varepsilon(\hat{t}_{\rm CO})}{\varepsilon(\hat{t}_{\rm ONe})}. \quad (6)$$

This ratio turns out to be $\tau_{\rm ONe}/\tau_{\rm CO} \approx 1.5$. Recalling that the fraction η of ONe white dwarfs for limiting magnitudes fainter than $25^{\rm mag}$ is typically 0.02 for the standard initial mass function and 0.01 for the biased initial mass function, the increment in the total optical depth due to ONe white dwarfs can be estimated to be

$$\frac{\Delta\tau}{\tau_0} \approx \eta \frac{\tau_{\rm ONe}}{\tau_{\rm CO}}, \quad (7)$$

which represents an increment of roughly 3% for the case in which a standard initial mass function is considered and a 2% increment for the case of the log-normal initial mass function. These results are in nice agreement with those previously presented in Fig. 2. On the other hand, when the magnitude cut is $30^{\rm mag}$ the fraction of ONe microlenses η increases significantly and, thus, the fractional increase of the optical depth due to ONe white dwarfs consequently increases, reaching values as high as 100%. This fact is responsible for the different behaviour of the deepest magnitude bins of the left panel of Fig. 2, which show the situation for the standard initial mass function. The biased initial mass function suppresses the formation of moderately massive ONe white dwarfs, and this is the reason why these faintest luminosity bins are not as populated as the equivalent bins for the case in which a standard mass function is considered.

In a second set of Monte Carlo calculations we have simulated the observational data obtained by the EROS team. We recall here that the EROS collaboration have not found any microlensing event towards the LMC and one candidate event towards the SMC. Adopting a standard halo model and assuming $\tau_{\rm SMC} = 1.4\tau_{\rm LMC}$, the EROS results imply an optical depth $\tau_0 = 0.36 \times 10^{-7}$ (Tisserand et al. 2006), which is four times smaller than that obtained by the MACHO team. Although it is expected that the value of the optical depth obtained from our simulations should be only slightly different, it is as well true that this may be a test of the robustness of our numerical procedures. In particular, the detection efficiency of both experiments is very different. Additionally the areas (and the number of objects) surveyed by both teams are different. The data results are summarized in Table 3. Our simulations show that the white dwarf population could account for a 35% of the optical depth found by the EROS team if a standard initial mass function is adopted, while for the non-standard initial mass function the contribution of the white dwarf population could be as large as 50%. On the other hand the expected number of objects has an upper limit of 1 for the standard initial mass function and 2 for the log-normal initial mass function. Both results are in agreement with the results of the EROS experiment. Again, as it was the case for the simulation of the MACHO experiment, the contribution of ONe white dwarfs is small. All in all, it seems that the microlensing optical depth obtained by the MACHO collaboration is a clear overestimate.

3.3. The Hubble Deep Field South

Kilic et al. (2005) have recently re-observed the Hubble Deep field south (HDF-S), and have found three white dwarf candidates among several faint blue objects which exhibit significant proper motion and, thus, are assumed to belong to the thick-disk or the halo populations. Consequently, we have also performed a series of Monte Carlo simulations in the direction of the HDF-S ($l = 328.25°$ $b = -49.21°$) for a small window of 4.062 arcmin^2. We have used the Johnson-Cousins *UBVRI* system instead of the WFPC2 photometry because the differences between both photometric systems is smaller than $0.02^{\rm mag}$ for the range of colors under study (Holtzman et al. 1995). Also, no reddening was applied to the synthetic white dwarf stars. Contrary to what has been done until now the results presented in this section are the average of 10^3 different realizations. Each of these realizations has been normalized to the local density of halo white dwarfs as previously described. The synthetic white dwarf population using this procedure is shown in the color-magnitude diagram of Fig. 4. In this figure we represent two typical simulations for the halo white dwarf population in the direction of the HDF-S for the two initial mass functions under study. As can be seen, the number of white dwarfs susceptible to be detected in the HDF-S survey – that is, those with I magnitude smaller than $27^{\rm mag}$ – is substantially larger for the log-normal initial mass function of Adams & Laughlin (1996) than for the standard initial mass function. Specifically, the average number of objects with $I < 27^{\rm mag}$ turns out to be 6 ± 2 for the case in which a standar initial mass function is adopted, while for the log-normal initial mass function this number is 110 ± 8. However, and in order to avoid confusion with blue extragalactic objects and main sequence stars, Kilic et al. (2005) restricted their search for white dwarfs candidates to colors in the range $V - I < 0.4$. Adding this new restriction we obtain that the expected number of white dwarfs should be 1 ± 1 for both initial mass functions. Although this result implies that both initial mass functions are compatible with the observations, the log-normal initial mass function

Table 3. Summary of the results obtained for the simulation of microlenses towards the LMC for the EROS model for an age of the halo of 14 Gyr, different model IMFs, and several magnitude cuts.

	Standard			AL		
Magnitude	17.5	22.5	27.5	17.5	22.5	27.5
$\langle N_{\rm WD}\rangle$	0 ± 1	0 ± 1	0 ± 1	1 ± 2	1 ± 2	0 ± 2
$\langle m\rangle$ $(M/M_\odot)$	0.607	0.595	0.622	0.631	0.634	0.642
$\langle \mu\rangle$ ($''$ yr^{-1})	0.013	0.011	0.008	0.034	0.025	0.010
$\langle d\rangle$ (kpc)	4.29	4.52	6.71	1.50	2.03	5.39
$\langle V_{\rm tan}\rangle$ (km s^{-1})	256	239	246	240	244	258
$\langle \hat{t}_{\rm E}\rangle$ (d)	64.9	77.0	89.7	37.9	45.3	74.8
$\langle \tau/\tau_0\rangle$	0.344	0.372	0.392	0.368	0.384	0.505

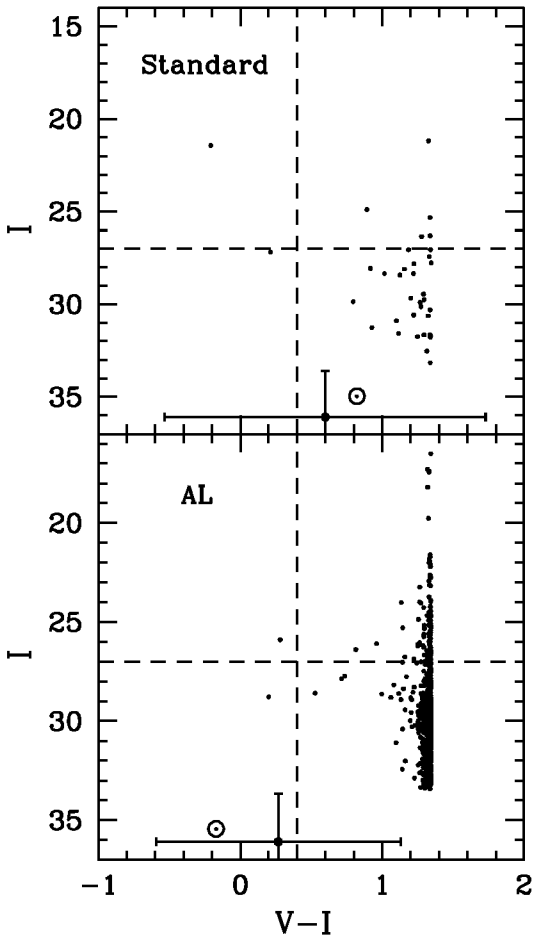

Fig. 4. Color-magnitude diagram for the white dwarf distribution (ONe white dwarfs are circled) for the HDF-S of two typical simulations. The dashed line respresents the HDF-S observation limit. Also represented is the average expected location within 1σ error of a typical ONe white dwarf. See text for details.

produces a large number of white dwarfs with colors in the interval $0.6 < V - I < 1.4$, which has no observational counterpart. Additionally, in Fig. 4 we also show the only one ONe white dwarf obtained for each one of these two typical simulations. In both cases its location is shown as an encircled dot in the color-magnitude diagram. It is worth mentioning that in most of the 10^3 realizations an ONe white dwarf is found, and thus we also show the average location of ONe white dwarfs in the color-magnitude diagram, along with the corresponding 1σ error bars. Note that in any case ONe white dwarfs are much fainter and bluer than normal CO white dwarfs, as it should be expected given that for a typical age of the halo most ONe white dwarfs have already reached the blue hook in the color-magnitude diagram.

3.4. The dark matter density

The results discussed so far indicate that, even in the case in which the contribution of ONe white dwarfs is taken into account, only a small fraction of the microlensing optical depth towards the LMC can be attributed to white dwarfs. We recall that if we adopt the microlensing optical depth of the MACHO experiment this contribution is nearly a 20% for the biased initial mass function of Adams & Laughlin (1996) and ~10% for the standard initial mass function. Besides, for a spherical isothermal halo model the microlensing optical depth towards the LMC is given by the expression (Alcock et al. 2000; Griest 1991):

$$\tau_{\rm LMC} = 5.1 \times 10^{-7} f \tag{8}$$

where f is the fraction of the halo mass that is made of lensing objects. Thus, the white dwarf population would contribute $f \approx 0.05$ to the mass of the halo in the most optimistic case.

However, we can go one step beyond using the results of our Monte Carlo simulations. In particular, we can compute the baryonic dark matter density in the form of white dwarfs using the $1/V_{\rm max}$ method. We proceed as follows. For each star of the sample we determine the maximum volume over which each star can contribute as a microlensing event using the expression

$$V_{\rm max} = \frac{\Omega}{3}(r^3_{\rm max} - r^3_{\rm min}) \tag{9}$$

where $r_{\rm max}$ is the radius of the volume in which we distribute the objects of our sample, which in our case is the radius of Galactic halo, and $r_{\rm min}$ is the minimum volume for which a white dwarf still belongs to the sample considering its apparent magnitude to be fainter than the adopted magnitude cut. Then, the number density of white dwarfs is

$$n = \sum_{i=1}^{N_{\rm obj}} \frac{1}{V_{{\rm max}_i}}. \tag{10}$$

Using this procedure we find that the contribution of white dwarfs to the baryonic dark matter would be roughly a 3% in the case in which a standard intial mass function is considered and nearly a 5% for the case in which the initial mass function of Adams & Laughlin (1996) is adopted.

Finally, from our Monte Carlo simulations we can also derive the *total* density of baryonic matter in the Galactic halo within 300 pc from the Sun in the form of main sequence stars, stellar remmants and in the corresponding ejected mass. We obtain $\rho_0 = 2.6 \times 10^{-4}\, M_\odot$ pc^{-3} for the standard initial mass function and $3.8 \times 10^{-3}\, M_\odot$ pc^{-3} for the log-normal intial mass function.

Table 4. Density of baryonic matter ($M_\odot/\mathrm{pc}^3$) in the Galactic halo within 300 pc from the Sun in the form gas returned to the interstellar medium (ISM) and in the form of white dwarfs (WD).

	Standard		AL	
	CO	ONe	CO	ONe
ISM	1.1×10^{-4}	6.4×10^{-6}	2.8×10^{-5}	3.5×10^{-5}
WD	5.4×10^{-5}	9.5×10^{-7}	9.2×10^{-4}	5.3×10^{-6}

The respective contributions of CO and ONe white dwarfs to the mass budget and of the mass returned to the interstellar medium are also shown in Table 4. Note that the total contribution of ONe white dwarfs is rather limited. The total density of baryonic matter obtained from our Monte Carlo simulations can be compared as well with the local dynamical matter density:

$$\rho_{\mathrm{DM}} = \frac{v_{\mathrm{rot}}^2}{4\pi G R_\odot^2}, \tag{11}$$

where v_{rot} is the rotation velocity of the Galaxy and $R_\odot$ is the Galactocentric distance. Thus, the fraction η of baryonic matter of the Galaxy resulting from the white dwarf population can be estimated. Our results indicate that η would be a modest 0.02 for the case in which a standard initial mass function is adopted, whereas a sizeable fraction of the baryonic matter, $\eta = 0.52$, can be accounted if the initial mass function of Adams & Laughlin (1996) is assumed.

4. Conclusions

We have analyzed the contribution of ONe white dwarfs to the MACHO content of the Galactic halo. We find that although ONe white dwarfs fade to invisibility very rapidly and, thus, they are good baryonic dark matter candidates, their contribution to the microlensing optical depth towards the LMC is rather limited. In particular, we have found that when the contribution of ONe white dwarfs is taken into account the microlensing optical depth does not increase significantly, independently of the adopted initial mass function. If the microlensing optical depth is adopted to be that of the MACHO experiment, $\tau_0 = 1.2\times10^{-7}$ (Alcock et al. 2000) – which probably is an overestimate – we find that the fraction of the microlensing optical depth due to the whole white dwarf population is at most ~13% in the case in which a standard initial mass function is adopted and ~19% if the log-normal initial mass function of Adams & Laughlin (1996) is considered. These values are roughly ~3% larger than those already found by García-Berro et al. (2004), who only considered the contribution of CO white dwarfs. We have also studied if some of the candidate white dwarfs of the Hubble Deep Field South could be ONe white dwarfs and we have found that most probably this is not the case. Finally, we have also discussed the contribution of the whole white dwarf population to the mass of the Galactic halo. We have found that this contribution is of the order of a modest 5% in the most optimistic case. All in all, we conclude that white dwarfs are not significant contributors to the mass of the Galactic halo.

Acknowledgements. Part of this work was supported by the MEC grants AYA05–08013–C03–01 and 02, by the European Union FEDER funds and by the AGAUR.

References

Adams, F. C., & Laughlin, G. 1996, ApJ, 468, 686
Alcock, C., Allsman, R. A., Alves, D., et al. 1995, ApJ, 454, L125
Alcock, C., Allsman, R. A., Alves, D., et al. 1997, ApJ, 486, 69
Alcock, C., Allsman, R. A., Alves, D. R., et al. 2000, ApJ, 542, 281
Althaus, L. G., García-Berro, E., Isern, J., Córsico, A. H., & Rohrmann, R. D., 2007, A&A, 465, 249
Becker, A. C. Rest, A. Stubbs, & C., et al. 2005, IAU Symp., 225, 357
Belokurov, V., Evans, N. W., & Le Du, Y. 2003, MNRAS, 341, 1373
Belokurov, V., Evans, N. W., & Le Du, Y. 2004, MNRAS, 352, 233
Binney, J., & Tremaine, H. 1987, Galactic Dynamics (Princeton: Princeton Univ. Press)
Canal, R., Isern, J., & Ruiz-Lapuente, P. 1997, ApJ, 488, L35
Chabrier, G., Segretain, L., & Méra, D. 1996, ApJ, 468, 21
Chabrier, G. 2004, ApJ, 611, 315
Charlot, S., & Silk, J. 1995, ApJ, 445, 124
Cutri, R. M., Skrutskie, M. F., van Dyk, S., et al. 2003, 2MASS All Sky Catalog of point sources, Univ. of Massachusetts and IPAC/California Institute of Technology
Dehnen, W. & Binney, J. 1998, MNRAS, 298, 387
Eisenstein, D. J., Liebert, J., Harris, H. C. at al. 2006, ApJS, 167, 40
Finley, D. S., Koester, D., & Basri, G. 1997, ApJ, 488, 375
García-Berro, E., Torres, S., Isern, J., & Burkert, A. 2004, A&A, 418, 53
Gates, E. I., & Gyuk, G. 2001, ApJ, 547, 786
Goldman, B., Afonso, A., Alard, Ch., et al. 2002, A&A, 389, 69
Griest, K. 1991, ApJ, 366, 412
Gyuk, G., Dalal, N., & Griest, K. 2000, ApJ, 535, 90
Hambly, N. C., Irwin, M. J., & MacGillivray, H. T. 2001, MNRAS, 326, 1295
Hansen, B. M. S. 1998, Nature, 394, 860
Holopainen, J., Flynn, C., Knebe, A., Gill, S. P., & Gibson, B. K. 2006, MNRAS, 368, 1209
Holtzman, J. A., Burrows, C. J., Casertano, S., et al. G. 1995, PASP, 107, 1065
Ibata, R. A., Richer, H. B., Gilliland, R. L., & Scott, D. 1999, ApJ, 524, L95
Iben, I., & Laughlin, G. 1989, ApJ, 341, 312
Isern, J., García-Berro, E., Hernanz, M. Mochkovitch, R., & Torres, S. 1998, ApJ, 503, 239
James, F. 1990, Comput. Phys. Commun., 60, 329
Kallivayalil, N., van der Marel, R. P., Alcock, C., et al. 2006, ApJ, 638, 772
Kerins, E., Evans N. W. 1998, ApJ503, 75
Kilic, M., Mendez, R. A., Von Hippel, T., & Winget, D. E. 2005, ApJ, 633, 1126
Klypin, A., Zhao, H., & Somerville, R. 2002, ApJ, 573, 597
Lasserre, T. Afonso. C., Albert, J. N., et al. 2001, A&A, 355, L39
Liebert, J., Bergeron, P., & Holberg, J. 2005, ApJS, 156, 47
Liebert, J., Dahn, C. C., & Monet, D. G. 1989, in White Dwarfs, ed. G. Wegner (Berlin: Springer), 15
Muraki, Y., Sumi, T., Abe, F., et al. 1999, Progr. Theor. Phys. Suppl., 133, 233
Navarro, J. F., Frenck, C. S., & White, S. D. M. 1997, ApJ, 490, 493
Paczyński, B. 1986, ApJ, 304, 1
Rahvar, S. 2005, MNRAS, 356, 1127
Sahu, K. 1994, Nature, 370, 275
Salaris, M., García-Berro, E., Hernanz, M., Isern, J. & Saumon, D. 2000, ApJ, 544, 1036
Scalo, J. 1998, in The Stellar Initial Mass Function, ed. G. Gilmore & D. Howell, PASP Conf. Ser. (San Francisco), 142, 201
Schmidt, M. 1968, ApJ, 151, 393
Silk, J. 2007, in The invisible universe: dark matter and dark energy, Proc. of the Third Aegean Summer School (Berlin: Springer Verlag), in press, [arXiv:astro-ph/0603209]
Tisserand, P., Le Guillou, L., Afonso, C., et al. 2006, [arXiv:astro-ph/0607207]
Torres, S., García-Berro, E., & Isern, J. 1998, ApJ, 508, L71
Udalski, A., Szymanski, M., Kaluzny, J., et al. 1994, Acta Astron., 44, 1
Vennes, S., Smith, R. J., Boyle, J., et al. 2002, MNRAS, 335, 673
Zhao, H. S. 1998, MNRAS, 294, 139